Global risk model for vector-borne transmission of Zika virus reveals the role of El Niño 2015

Cyril Caminade[a,b,1], Joanne Turner[a], Soeren Metelmann[b,c], Jenny C. Hesson[a,d], Marcus S. C. Blagrove[a,b], Tom Solomon[b,e], Andrew P. Morse[b,c], and Matthew Baylis[a,b]

[a]Department of Epidemiology and Population Health, Institute of Infection and Global Health, University of Liverpool, Liverpool CH64 7TE, United Kingdom; [b]Health Protection Research Unit in Emerging and Zoonotic Infections, University of Liverpool, Liverpool L69 3GL, United Kingdom; [c]Department of Geography and Planning, School of Environmental Sciences, University of Liverpool, Liverpool L69 7ZT, United Kingdom; [d]Department of Medical Biochemistry and Microbiology, Zoonosis Science Center, Uppsala University, Uppsala 751 23, Sweden; and [e]Department of Clinical Infection, Microbiology and Immunology, Institute of Infection and Global Health, University of Liverpool, Liverpool L69 7BE, United Kingdom

Edited by Anthony A. James, University of California, Irvine, CA, and approved November 14, 2016 (received for review September 2, 2016)

Zika, a mosquito-borne viral disease that emerged in South America in 2015, was declared a Public Health Emergency of International Concern by the WHO in February of 2016. We developed a climate-driven R_0 mathematical model for the transmission risk of Zika virus (ZIKV) that explicitly includes two key mosquito vector species: *Aedes aegypti* and *Aedes albopictus*. The model was parameterized and calibrated using the most up to date information from the available literature. It was then driven by observed gridded temperature and rainfall datasets for the period 1950–2015. We find that the transmission risk in South America in 2015 was the highest since 1950. This maximum is related to favoring temperature conditions that caused the simulated biting rates to be largest and mosquito mortality rates and extrinsic incubation periods to be smallest in 2015. This event followed the suspected introduction of ZIKV in Brazil in 2013. The ZIKV outbreak in Latin America has very likely been fueled by the 2015–2016 El Niño climate phenomenon affecting the region. The highest transmission risk globally is in South America and tropical countries where *Ae. aegypti* is abundant. Transmission risk is strongly seasonal in temperate regions where *Ae. albopictus* is present, with significant risk of ZIKV transmission in the southeastern states of the United States, in southern China, and to a lesser extent, over southern Europe during the boreal summer season.

Zika virus | R_0 model | El Niño | *Ae. aegypti* | *Ae. albopictus*

Zika virus (ZIKV) is an emerging mosquito-borne virus that infects and causes disease in humans. Approximately 80% of infections are asymptomatic; the 20% of clinically affected people mostly experience mild symptoms, such as fever, arthralgia, and rash (1). A small proportion is believed, however, to develop a paralytic autoimmune disease called Guillain–Barré syndrome (2, 3). There is also evidence that the infection of women during a critical part of pregnancy can lead to the development of microcephaly in the unborn child (4, 5). The recent discovery of ZIKV in South America and a surge in the number of reports of Guillain–Barré syndrome and microcephaly cases in the region led the WHO to announce a Public Health Emergency of International Concern on February 1 of 2016.

ZIKV was first isolated in Uganda from monkeys in 1947 and *Aedes africanus* mosquitoes in 1948 (6). Several other mosquito species (mostly of the genus *Aedes*) have been implicated as ZIKV vectors. Globally, the most important is the Yellow Fever mosquito, *Aedes aegypti* (7), which is widespread in tropical regions of the world. A second vector is the Asian tiger mosquito, *Aedes albopictus* (8), one of the world's most invasive mosquito species. It occurs in both tropical and temperate regions, often together with *Ae. aegypti*, but also, extends farther north into temperate countries. Other *Aedes* species may be locally important, such as *Aedes hensilli*, which is considered to have been the primary vector in the Zika outbreak in French Polynesia in 2007 (1, 9).

The risk of spread of an infectious disease can be described by its basic reproduction ratio (R_0) defined as the average number of secondary infections arising from a typical primary infection in an otherwise fully susceptible population. R_0 has an important threshold value: a value above one indicates that the pathogen could spread if it were introduced, resulting in a minor or major outbreak depending on the size of R_0, whereas a value below one indicates that pathogen transmission would be insufficient to produce a major outbreak. Mathematical formulations of R_0 exist for several vector-borne diseases (VBDs), including those with one host and one vector [such as malaria (10)] and those with two hosts and one vector [such as zoonotic sleeping sickness (11) and African horse sickness (12)]. Relatively little attention has been paid to developing mathematical formulations of R_0 where there are two vector species and either one or multiple host species (13). Consideration of two vector species in the R_0 formulation is essential where two vectors have different epidemiological parameters. It also allows for the estimation of R_0 where the two species co-occur and primary infections in one species can lead to secondary infections in the second.

Ae. aegypti and *Ae. albopictus* seem to have different susceptibilities to ZIKV (7, 14–16), feeding rates, and feeding preferences (17, 18). *Ae. aegypti* feeds more often and almost exclusively on humans, and it is, therefore, an extremely efficient transmitter of human viruses. *Ae. albopictus* feeds less frequently and on a broader range of hosts, and it is, therefore, less likely to both acquire and transmit a human virus. Given equal mosquito and human densities, regions with *Ae. aegypti* are, therefore, theoretically

Significance

This study quantifies the impact of climate variability on Zika virus (ZIKV) transmission by two mosquito vectors with distinct characteristics: *Aedes aegypti and Aedes albopictus*. Observed climate data were used to dynamically drive a two vectors–one host R_0 epidemiological model. Our modeling results indicate that temperature conditions related to the 2015 El Niño climate phenomenon were exceptionally conducive for mosquito-borne transmission of ZIKV over South America. The virus is believed to have entered the continent earlier in 2013. This finding implicates that such a large ZIKV outbreak occurred not solely because of the introduction of ZIKV in a naive population, but because the climatic conditions were optimal for mosquito-borne transmission of ZIKV over South America in 2015.

Author contributions: C.C., T.S., A.P.M., and M.B. designed research; C.C., J.T., and S.M. performed research; J.T. developed the analytical framework of the model; C.C., J.T., S.M., and M.S.C.B. analyzed data; J.C.H. conducted the large literature review; and C.C. and M.B. wrote the paper with input from all coauthors.

The authors declare no conflict of interest.

This article is a PNAS Direct Submission.

Freely available online through the PNAS open access option.

Data deposition: Model output is publicly available on the Open Science framework platform at osf.io/ubwya/.

[1]To whom correspondence should be addressed. Email: Cyril.Caminade@liverpool.ac.uk.

This article contains supporting information online at www.pnas.org/lookup/suppl/doi:10.1073/pnas.1614303114/-/DCSupplemental.

expected to have a higher R_0 for ZIKV than regions with *Ae. albopictus*, but because *Ae. albopictus* extends beyond the range of *Ae. aegypti* into more temperate regions, it is essential that both are included in global models of ZIKV transmission risk.

The risk of transmission of a mosquito-borne virus and hence, its R_0 are also highly sensitive to climate (19). Temperature and rainfall influence the abundance and seasonality of mosquitoes. Furthermore, temperature has a major effect on the capacity of a population of mosquitoes to transmit virus. This capacity is influenced by the mean number of blood meals in a typical mosquito's remaining lifespan after the point at which it becomes infectious (20), which is determined by the combined effects of the feeding frequency (estimated by biting rates) and longevity of the mosquitoes (estimated from mortality rates) and the time required for development of virus inside a mosquito [the extrinsic incubation period (EIP)]. All three of these variables are highly sensitive to environmental temperature conditions.

Here, we develop a global R_0 model for ZIKV that explicitly includes two vector species and one host and considers the influence of climate dynamically. First, we extend a recently developed two-vector mathematical framework for an animal VBD (13) to ZIKV. Second, we parameterize the model using recently published estimates of the global distribution of *Ae. aegypti* and *Ae. albopictus* as well as the temperature-sensitive virus transmission variables described above. Third, we drive the model using global observation-based historical climate data to derive global and seasonal estimates of the R_0 of ZIKV that describe transmission risk by one, the other, and both vectors where they co-occur.

Our model considers risk of transmission by vectors only. There is strong evidence that ZIKV can also be transmitted sexually (21). Although the number of confirmed cases to date is very small relative to the number of cases believed to have been caused by mosquito bites, it does allow the spread of ZIKV in regions where mosquito vectors are absent. If the risk of sexual transmission remains small, however, our model indicates where and when the greatest risks of vector transmission occur, where vector control measures may be most usefully implemented, and when and where health professionals should communicate potential ZIKV threat to infected travelers returning from ZIKV-endemic countries.

Results

Our R_0 model output (Fig. 1 *A* and *B*) captures well the observed largely tropical distribution of ZIKV transmission (Fig. 1*C*). Since the 1950s, ZIKV transmission or seropositivity has been reported in several African countries, Pakistan, India, southeastern Asia, and parts of Oceania (22), and it recently spread in 2015 and 2016 to Latin American countries, Florida, Thailand, and the Philippines (Fig. 1*C*), where importantly, large R_0 values are simulated. It has been speculated that the epidemiologically naïve population of people in South America may account for the size of the outbreak there. Although this statement is very likely true, our model also finds the average R_0 of ZIKV to be greater in South America than in any other region of the world. Other areas with high values of R_0 are some African countries (Côte d'Ivoire, Central African Republic, Nigeria, Kenya, Tanzania, and Uganda) and Asian countries (India, Vietnam, the Philippines, Singapore, parts of Malaysia and Indonesia, and Thailand), where ZIKV circulation was also previously reported (7, 8, 22–29). The model finds southern and southeastern Asia to be suitable for ZIKV transmission. ZIKV was first identified in Asia nearly 50 y ago (28), but there have not been significant outbreaks recorded. The model seems to underpredict for Egypt, because it does not find Egypt to be suitable for ZIKV transmission, although seropositive people have been reported there. Nevertheless, the prevalence in Egypt is believed to be very low (30).

The R_0 model output is further validated against other published estimates of R_0 for Rio de Janeiro, Brazil and Colombia as a whole (Fig. 2). The minimum; 25th, 50th, and 75th percentiles; and maximum R_0 values simulated for Rio de Janeiro (0, 3.4, 3.9, 4.3, and 5, respectively) are very similar to estimates in ref. 31 (0, 3.2, 3.8, 4, and 4.6, respectively). The simulated R_0 values for Colombia

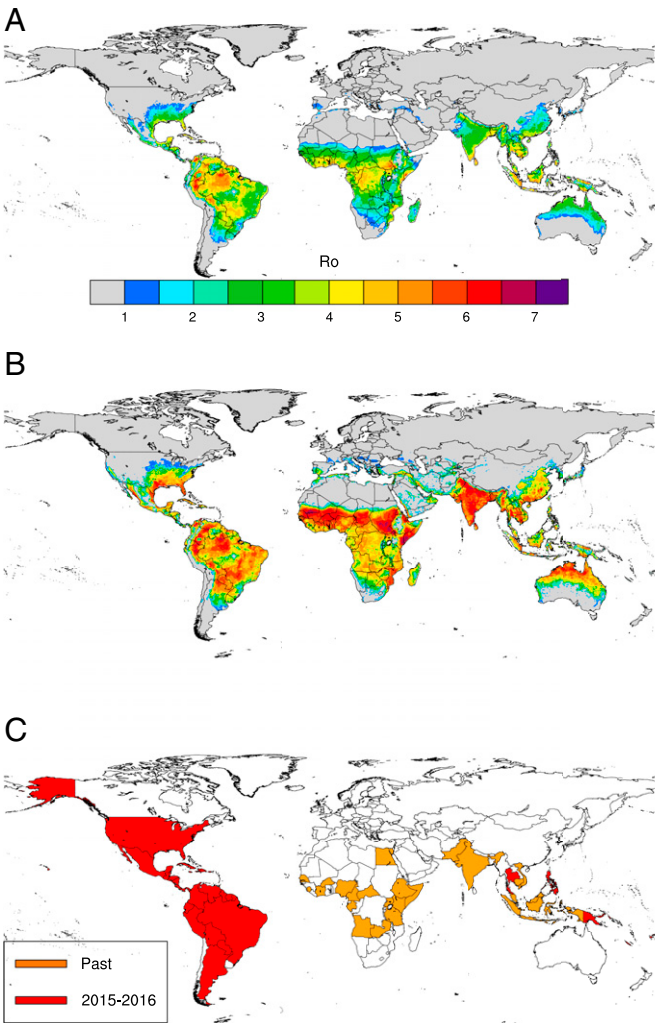

Fig. 1. Observed and simulated ZIKV distribution. (*A*) Mean annual R_0 (calculated over the period 1980–2015), (*B*) annual R_0 peak that represents the largest monthly value over the whole time period (1980–2015), and (*C*) past and recent (2015–2016) countries with reported ZIKV circulation.

range from 0 to 6.9, with a median value of 4.1. These values are also in good agreement with preliminary R_0 estimates for ZIKV in Colombia (3, 3.9, and 6.6) (32). The climate data are unfortunately too spatially coarse to obtain R_0 estimates for small islands in Oceania, where Zika outbreaks were also reported in the last decade. Furthermore, if one assumes that ZIKV transmission might occur where dengue virus transmission was reported because of the similarity of both viruses and their mosquito vectors, the ZIKV R_0 model captures about 96% of dengue occurrence points as reported in ref. 33 (*SI Appendix*, Fig. S1 and Table S1).

Next, we investigated the effect of seasonal change in climate on the risk of ZIKV transmission. Our R_0 model shows that boreal summer temperature conditions lead to increased R_0 values over temperate regions where both vectors (or only *Ae. albopictus*) are present (*SI Appendix*, Fig. S2). Thus, the model outputs suggest that the environmental conditions might be suitable for ZIKV transmission to occur over a wider geographical range than has currently been observed (Fig. 1*A*), particularly when considering the seasonal peak in R_0 (Fig. 1*B*). Over the South American continent, R_0 values are large all year and peak during the boreal winter and spring (*SI Appendix*, Fig. S3). In Africa, the largest R_0 values are simulated over southern Africa during boreal winter and the Sahelian region during boreal summer and fall (*SI Appendix*, Fig. S4), which correspond to the peak of the rainy season over

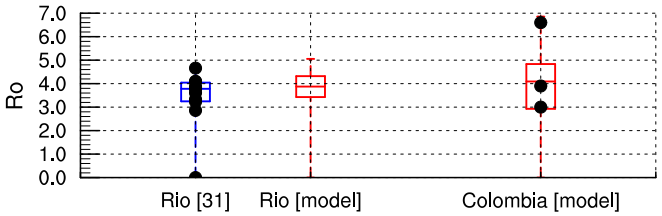

Fig. 2. Comparison of simulated R_0 with other published estimates. Box and whisker plot of simulated R_0 (red) vs. other published estimates (blue box and whisker plot and black dots for single-point estimates) for Rio de Janeiro (31) and Colombia (32). The box and whisker plot depicts the minimum; 25th, 50th, and 75th percentiles; and maximum across the ensemble of values. Simulated distributions are based on closest grid point for Rio de Janeiro and all country values for Colombia over the 1950–2015 period.

these regions. Over Asia, R_0 values are relatively large all year in Oceania, whereas a clear peak in R_0 is shown during boreal summer and fall over India, Vietnam, Laos, and Cambodia (*SI Appendix*, Fig. S5). During boreal summer, a large increase in R_0 is simulated over the southeastern states of the United States (*SI Appendix*, Fig. S6), and smaller increases are simulated over southern Europe (*SI Appendix*, Fig. S7) and southern China (*SI Appendix*, Fig. S5). The large R_0 summer values over the southeastern states of the United States are because of both very conducive temperature conditions and the spatial overlap of *Ae. albopictus* and *Ae. aegypti* (*SI Appendix*, Fig. S8). Therefore, our model indicates that there is a large potential risk of ZIKV transmission in the southeastern United States and to a lesser extent, over southern China and southern Europe in boreal summer. This signal mainly relates to the presence of the highly invasive *Ae. albopictus* in temperate regions (*SI Appendix*, Fig. S8) as well as higher biting rates (*SI Appendix*, Fig. S9), lower EIPs (*SI Appendix*, Fig. S10), and lower mortality rates (*SI Appendix*, Fig. S11) during the warm season.

The modeling framework also allows investigation of the respective contributions of *Ae. aegypti* and *Ae. albopictus* to the total R_0 burden (*SI Appendix*, Fig. S12). Given the selected parameter settings, which are based on the published literature, *Ae. aegypti* is responsible for >90% of ZIKV transmission risk in the tropics, whereas *Ae. albopictus* seems to make a smaller contribution (less than 10%). *Ae. albopictus* is, however, the main vector responsible for ZIKV transmission risk in temperate areas, such as the northern United States and southern Europe (*SI Appendix*, Fig. S12).

VBDs are not just affected by seasonal variations in climate; extreme climatic anomalies can also favor epidemics. One of the strongest El Niño events ever recorded occurred in 2015–2016, and there have been concerns about its possible impact on VBD burden (34) and agricultural production worldwide. El Niño events are characterized by the movement of warmer than average sea surface temperatures across the central Pacific basin and associated with warmer temperature conditions over the Tropics and rainfall anomalies that vary greatly by region and season. To investigate the impact of El Niño on potential ZIKV transmission risk at a global scale, we derived the R_0 relative anomaly for 2015 (Fig. 3*A*). Large positive anomalies in R_0 are simulated over the Tropics, meaning that climate conditions were particularly conducive for ZIKV transmission in 2015 relative to the long-term average. This signal can be seen over South America (especially Colombia and Brazil) but also, in Africa (with the largest anomaly shown over Angola), southern India, Southeast Asia, and Oceania. Although intense ZIKV transmission was only reported over Central America and South America in 2015, the virus is believed to have entered the region in 2013 (35). Standardized model anomalies calculated for the South American continent further reveal that 2015 was the year with the highest R_0 value (exceeding 2 SDs) over the whole 66-y time period (Fig. 3*B*). This R_0 maximum is mainly related to simulated maximum biting rates, minimum EIPs, and mortality rates in 2015 (*SI Appendix*, Figs. S13 and S14). A large positive anomaly is also shown for the 1997–1998 El Niño before ZIKV was introduced to the South American continent. Therefore, our model indicates that the 2015 El Niño event, superimposed on the long-term global warming trend, has had an important amplification effect through its impacts on mosquito vector and their overall ability to transmit virus.

Discussion

The model provided interesting insights into the spatiotemporal distribution of potential disease transmission risk, permitted the relative contributions of the two main disease vectors to be quantified, and implicates the current El Niño in playing an important amplification role. Importantly, we show that warm temperature conditions associated with the current El Niño climate phenomenon superimposed on the warming trend were exceptionally conducive for mosquito-borne transmission of ZIKV in 2015 over the South American continent. The conducive temperature conditions in 2015 over South America can be related to the superposition of climate change and decadal and year to year variability (36). Similarly, R_0 modeling work for the risk of bluetongue, an animal VBD that emerged in northern Europe in 2006, highlighted that temperature conditions in northern Europe in that particular year were also exceptionally conducive for disease transmission (37). Other notable impacts of El Niño 2015–2016 are historical droughts impacting food security in Ethiopia and southern Africa and forest fires in California, Canada, Malaysia, and Indonesia. The number of dengue cases in India in 2015 was the largest recorded (38). Interestingly, our model finds one of the largest 2015 R_0 anomalies for ZIKV in Africa to be centered on Angola. Although ZIKV has not

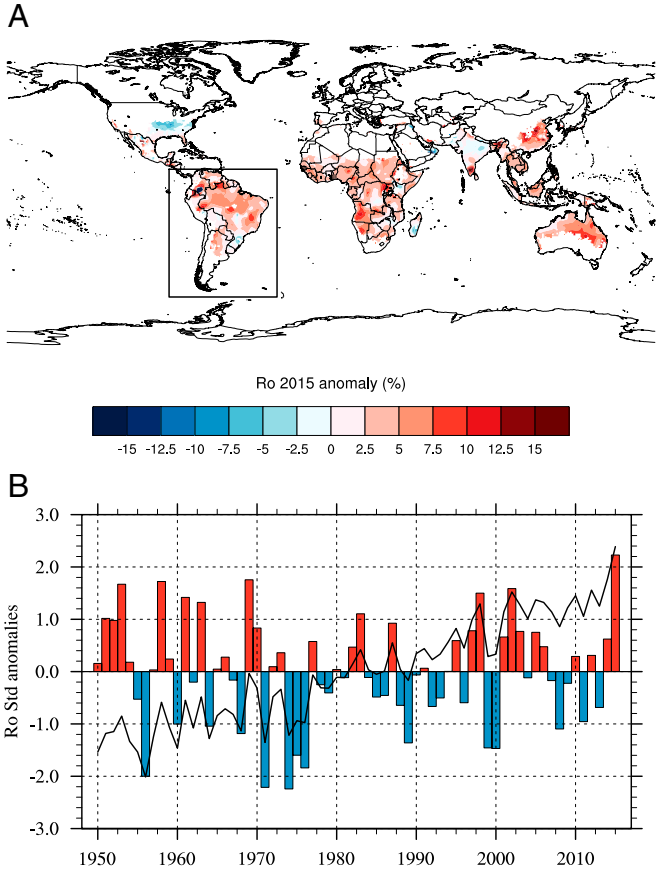

Fig. 3. ZIKV transmission risk anomalies. (*A*) Annual R_0 2015 anomaly (percentage) with respect to the 1950–2015 period. (*B*) Standardized R_0 anomalies with respect to the 1950–2015 period. The indices have been calculated for the South American continent; *A* shows the spatial domain definition. The solid line and the colored bars depict raw and linearly detrended anomalies, respectively.

been recently reported, Angola is currently experiencing a large outbreak of Yellow Fever transmitted by *Ae. aegypti*, and we speculate, therefore, that this outbreak might also have been favored by El Niño conditions. This finding raises additional concerns about the impact of large El Niño events on VBD risk in a future warmer, more connected world with increasing levels of drug and insecticide resistance. Flaviviruses, in general, should have a promising future (39).

Our results corroborate that *Ae. aegypti*, likely because of its anthropophilic behavior and its aggressiveness, is a larger threat than *Ae. albopictus* for ZIKV transmission worldwide. However, the threat posed by *Ae. albopictus* is not negligible, especially during the warm season in temperate regions, and the overlap of both vector species produces the largest R_0 values. Similarly, in Europe in recent years, *Ae. albopictus* was responsible for a small number of autochthonous cases of chikungunya and dengue in Italy, southern France, and Croatia, whereas *Ae. aegypti* was responsible for more than 2,000 cases of dengue on the island of Madeira in 2012 (40, 41). Consequently, there is a need to focus disease preparedness measures or vector control interventions primarily in regions infested by *Ae. aegypti* or where both vectors co-occur.

The simulated spatial distribution of ZIKV is similar to other published estimates, which used environmental covariates and the boosted regression tree method to estimate environmental suitability for ZIKV at global scale (42) or a one-host, one-vector R_0 modeling approach to derive attack rates for Latin America (43). Our model framework further allowed for exploring of spatial and temporal changes in potential disease risk. We showed the potential of ZIKV transmission during boreal summer over the southeastern states of the United States as previously considered by others (44). Autochthonous transmission of ZIKV was observed in Florida in the summer of 2016. However, only a few cases were reported so far; because there is large proportion (80%) of asymptomatic infections with ZIKV, more people might be infected without showing any clinical signs.

There are several caveats in our modeling framework that need to be mentioned. First, we did not consider sexual transmission of ZIKV, because it likely plays a very minor role in the overall amount of transmission. Second, we only considered the risk posed by *Ae. aegypti* and *Ae. albopictus*, believed to be the main competent vectors of ZIKV (and certain other arboviruses, such as dengue and chikungunya viruses). However, other *Aedes* species can transmit ZIKV locally (such as *Ae. hensilli* in Pacific islands and *Ae. africanus* in parts of Africa). There is also a debate about the capacity of the geographically widespread *Culex quinquefasciatus* vector to transmit ZIKV (45–47). However, most recent studies are showing poor or no competence of this species to transmit ZIKV. Our model might, therefore, underestimate R_0 in some localities where vectors other than *Ae. aegypti* or *Ae. albopictus* are present. Our mathematical framework can be readily extended to include additional vectors, but limitations arise from the lack of detailed distribution and epidemiological data for these species. There is an urgent need for additional studies on vectors of ZIKV and their distribution, abundance, and transmission parameters. Third, estimates of vector to host ratios for *Ae. aegypti* and *Ae. albopictus* were approximated from probability of occurrences, because they were limited by the large spatial and temporal differences in published field studies. Additional estimates of mosquito densities in different demographic and geographic settings, preferably with standardized methods (48), will be highly useful to improve and upscale mechanistic spatiotemporal risk models. ZIKV EIPs were approximated by dengue virus estimates in our study, because they were similar in high-temperature settings (7). Better estimates of the dependency of the EIP of ZIKV to temperature, especially in the lower and higher temperature tails of the distribution, will be highly valuable for additional model refinement.

Our R_0 model presents the risk of transmission given the introduction of virus in a fully susceptibility population. It does not address the potential of the pathogen and the vectors to spread via tourism and trade or the risk of transmission in populations that have already been exposed to ZIKV. Recent modeling work suggests that the ZIKV epidemic in Latin America should be over in 3 y maximum and that acquired herd immunity will likely cause a delay of more than a decade until large epidemics reemerge (49). India, China, Indonesia, the Philippines, and Thailand have been estimated at risk for mosquito-borne ZIKV infection because of the large volume of travelers arriving from affected areas in Latin America (50). Furthermore, socioeconomic factors (such as health service per capita, urbanization, and vulnerability indices) should be included in assessments of the full impact of Zika in future studies. Our model uses recently published studies by the medical, biological, and entomological communities; it benefits from statistical (51) and mathematical (13) modeling techniques and recent environmental datasets produced by the National Oceanic and Atmospheric Administration (52, 53). This fact underlines the importance of taking multidisciplinary approaches to address and anticipate the health and food security challenges to come.

Materials and Methods

R_0 Model Design. To calculate R_0 for ZIKV transmission, we adapted the two hosts–two vectors expression derived from ref. 13. This expression is suitable for pathogens, including bluetongue virus, that have two main hosts and two main vectors with different feeding preferences. In the case of ZIKV, there is one main host (i.e., humans) capable of transmitting the virus. Therefore, we prevented the second host from contracting and transmitting the infection. However, because *Ae. aegypti* and *Ae. albopictus* feed to different extents on humans, we retained the measures of feeding preference. In addition, because infection with ZIKV is not associated with mortality, the standard pathogen-induced mortality rate (d) was set to zero. The resulting expression is

$$R_0 = \sqrt{\widetilde{R_{11}} + \widetilde{R_{22}}}, \qquad [1]$$

where

$$\widetilde{R_{11}} = \left(\frac{b_1\beta_1 a_1^2}{\mu_1}\right)\left(\frac{\nu_1}{\nu_1+\mu_1}\right)\left(\frac{\phi_1^2 m_1}{r}\right) \text{ and}$$

$$\widetilde{R_{22}} = \left(\frac{b_2\beta_2 a_2^2}{\mu_2}\right)\left(\frac{\nu_2}{\nu_2+\mu_2}\right)\left(\frac{\phi_2^2 m_2}{r}\right).$$

R_{ij} is the average number of infectious vectors of type i produced by an infectious vector of type j; one stands for *Ae. aegypti*, and two stands for *Ae. albopictus*. As a result of the second host being noninfectious, the between-species terms R_{12} and R_{21} are eliminated from R_0 (additional details are given in *SI Appendix*). In fact, this expression for R_0 is true for any number of hosts, providing that only one of them is a true host (i.e., capable of transmitting the infection). Biting rates (a), mortality rates (μ), and EIPs ($eip = 1/\nu$) for both vector species are the only parameters dynamically relying on temperature data. These dependencies to temperature were calculated based on published evidence from the literature (Table 1 and *SI Appendix*, Fig. S15). Vector preferences (ϕ), transmission probabilities (from vector to host b and host to vector β), and ZIKV recovery rate (r) were assumed to be constant, and they were derived from recently published estimates for ZIKV or dengue virus if they were not available (Table 1).

Vector to host ratios (m_1 and m_2) were derived from published probability of occurrence ($prob_1$ and $prob_2$) at global scale (51). Given the large differences in mosquito density estimates published in the literature for different regions and seasons (48), these probabilities of occurrences (0–1) have been arbitrarily linearly rescaled to range between zero and a maximum estimate of vector to host ratio following the work in ref. 37. This maximum was estimated as an order of magnitude (*SI Appendix*, Fig. S16) using the maximum ZIKV R_0 value to calibrate it. A maximum R_0 value of 6.6 was reported in ref. 32 for Colombia during the outbreak. This maximum R_0 value is reached when the vector to host ratio value reaches about 1,000 in the model between 30 °C and 37 °C (*SI Appendix*, Fig. S16*C*). This constraint is on the maximum solely; however, the model reproduces well the distribution of R_0 values with respect to other published estimates (Fig. 2). Lower values for m are generally reported by entomologists [10 is a commonly reported value (48)]. However, this value depends on the selected field method to estimate m. Values of 52 *Aedes* mosquitoes per person per hour have been reported in Macao using human baits, 1.8 mosquitoes per hour have been reported using Centers for Disease Control and Prevention (CDC) traps, and 110 mosquitoes per hour have been reported using aspirators (54). Because both *Aedes* species are active from dawn to dusk (e.g., over 12 h maximum, with a peak of activity in the early morning and late afternoon), this is equivalent to 624, 21.6, and 1,320 mosquitoes per day, respectively, thus including the selected maximum if we assume that a trap

Table 1. R_0 model parameter settings—an index of 1 denotes *Ae. aegypti* and an index of 2 denotes *Ae. albopictus*

Symbol	Description	Constant/formula	Comments	Refs.
$*a_1$	Biting rates (per day)	$a_1 = 0.0043T + 0.0943$	The linear dependency to temperature was based on estimates for *Ae. aegypti* in Thailand; biting rates for *Ae. albopictus* were halved based on observed feeding interval data (18)	58, 59
$*a_2$		$a_2 = 0.5 \times a_1$		
ϕ_1	Vector preferences (0–1)	$\phi_1 = 1[0.88–1]$	Most studies show that *Ae. aegypti* mainly feeds on humans; *Ae. albopictus* can feed on other wild hosts (cats, dogs, swine...), and large differences are shown for feeding preference between urban and rural settings for this species	17, 54, 60–65
ϕ_2		$\phi_2 = 0.5[0.24–1]$		
b_1	Transmission probability—vector to host (0–1)	$b_1 = 0.5[0.1–0.75]$	Based on dengue parameters—estimates from a mathematical review study	66
b_2		$b_2 = 0.5[0.1–0.75]$		
β_1	Transmission probability—host to vector (0–1)	$\beta_1 = 0.1$	Recent laboratory experiment studies generally show low transmission efficiency (in saliva) for various vector/ZIKV strain combinations (South America and Africa); estimates from ref. 15 were used in the final model version	14–16
β_2		$\beta_2 = 0.033$		
$*\mu_1$	Mortality rates (0–1 per day)	$\mu_1 = 1/(1.22 + \exp(-3.05 + 0.72T)) + 0.196$ if $T < 22$ °C	Mortality rates were derived for both mosquito vectors from published estimates based on both laboratory and field data	67
$*\mu_2$		$\mu_1 = 1/(1.14 + \exp(5.14–1.3T)) + 0.192$ if $T \geq 22$ °C		
		$\mu_2 = 1/(1.1 + \exp(-4.04 + 0.576T)) + 0.12$ if $T < 15$ °C		
		$\mu_2 = 0.000339T^2 - 0.0189T + 0.336$ if 15 °C $\leq T < 26.3$ °C		
		$\mu_2 = 1/(1.065 + \exp(32.2–0.92T)) + 0.0747$ if $T \geq 26.3$ °C		
$*eip_1$	EIP (days)	$eip_1 = 1/\nu_1 = 4 + \exp(5.15–0.123T)$	EIPs for dengue were used because estimates for ZIKV were only available at a single temperature; 50% (100%) of *Ae. aegypti* mosquitoes were infected by ZIKV after 5 d (10 d) at 29 °C (7). An EIP longer than 7 d was reported in ref. 15 at similar temperature. Model estimates for dengue suggest $eip_1 \sim$ 8–9 d at 29 °C. The 1.03 multiplying factor for *Ae. albopictus* was derived from ref. 67	68
$*eip_2$		$eip_2 = 1/\nu_2 = 1.03(4 + \exp(5.15–0.123T))$		
m_1	Vector to host ratios	$m_1 = 1{,}000 \times prob_1$	m was derived as the product of a constant with probability of occurrences published at global scale for both mosquito vectors; *Materials and Methods* has additional details	51
m_2		$m_2 = 1{,}000 \times prob_2$		
r	Recovery rate (per day)	$r = 1/7$		69

T, temperature.
*Parameters that are dynamically simulated in space and time over the whole time period.

is a potential host. Biting rate estimates for *Ae. aegypti* of about 150 bites per person per day were reported for Thailand over a 7-mo period (55). In Macao, biting rates were reported to range between 94 and 314 bites per person per day (54). Our estimates of ($m \times a$) range between 100 and 250 bites per person per day for *Ae. aegypti* and between 25 and 125 bites per person per day for *Ae. albopictus* if we assume $m = 1{,}000$ (*SI Appendix*, Fig. S17).

The percentages of R_0 attributed to *Ae. aegypti* (R_{11}/R_0^2) and *Ae. albopictus* (R_{22}/R_0^2) were derived from Eq. **1**, which can be rewritten as $1 = 100\% = R_{11}/R_0^2 + R_{22}/R_0^2$. An explicit mathematical derivation of the R_0 model is provided in *SI Appendix*; parameter setting details and the publication references used to estimate them are shown and discussed in Table 1.

R_0 Model Integration and Driving Datasets. The Zika R_0 model is dynamic, meaning that some epidemiological parameters are varying in both space and time from 1948 to 2015. The model runs on a monthly time step. To incorporate rainfall seasonality effects, we used a criterion derived for malaria in Africa within the Mapping Malaria Risk in Africa project framework [e.g., "80 mm per month for at least five months for stable transmission" (56)]. If the criterion was not met, we assumed that $R_0 = 0$ for a particular location and month. All spatially varying parameters were interpolated to the temperature data grid.

For temperature, we used gridded data, which combine station data from the Global Historical Climatology Network version 2 with the Climate Anomaly Monitoring System (52). This monthly temperature dataset is available at 0.5° × 0.5°-square resolution at global scale for the period 1948–2015. For rainfall, we used the Global Precipitation Climatology Centre global rainfall data available at similar spatial and time resolution for the same time period (53).

R_0 Model Validation. Countries with active transmission of ZIKV (Fig. 1*C*) were obtained from the CDC at www.cdc.gov/zika/geo/active-countries.html and the European Center for Disease Prevention and Control at ecdc.europa.eu/en/healthtopics/zika_virus_infection/zika-outbreak/pages/zika-countries-with-transmission.aspx. Historical circulation of ZIKV at country scale (including seroprevalence estimates) was derived from refs. 22 and 57. Baseline R_0

estimates for Rio de Janeiro (Fig. 2) were mathematically derived from reported cases provided by the Brazilian Notifiable Information System (31). R_0 estimates for Colombia (Fig. 2) were mathematically derived from reported cases provided by the Instituto Nacional de Salud de Bogotá (32).

Supplementary Information. Additional details about the model design, the model validation, and additional analysis are provided in *SI Appendix*.

ACKNOWLEDGMENTS. The research was funded by the National Institute for Health Research (NIHR) Health Protection Research Unit in Emerging and Zoonotic Infections at the University of Liverpool in partnership with Public Health England (PHE) and Liverpool School of Tropical Medicine. C.C. acknowledges support from The Farr Institute for Health Informatics Research through Medical Research Council Grant MR/M0501633/1. The views expressed are those of the authors and are not necessarily those of the National Health Service, the NIHR, the Department of Health, or PHE.

1. Duffy MR, et al. (2009) Zika virus outbreak on Yap Island, Federated States of Micronesia. *N Engl J Med* 360(24):2536–2543.
2. Musso D, Nilles EJ, Cao-Lormeau VM (2014) Rapid spread of emerging Zika virus in the Pacific area. *Clin Microbiol Infect* 20(10):O595–O596.
3. Hazin AN, et al.; Microcephaly Epidemic Research Group (2016) Computed tomographic findings in microcephaly associated with Zika virus. *N Engl J Med* 374(22):2193–2195.
4. Mlakar J, et al. (2016) Zika virus associated with microcephaly. *N Engl J Med* 374(10):951–958.
5. de Paula Freitas B, et al. (February 9, 2016) Ocular findings in infants with microcephaly associated with presumed Zika virus congenital infection in Salvador, Brazil. *JAMA Ophthalmol*, 10.1001/jamaophthalmol.2016.0267.
6. Dick GWA, Kitchen SF, Haddow AJ (1952) Zika virus. I. Isolations and serological specificity. *Trans R Soc Trop Med Hyg* 46(5):509–520.
7. Li MI, Wong PS, Ng LC, Tan CH (2012) Oral susceptibility of Singapore Aedes (Stegomyia) aegypti (Linnaeus) to Zika virus. *PLoS Negl Trop Dis* 6(8):e1792.
8. Grard G, et al. (2014) Zika virus in Gabon (Central Africa)–2007: A new threat from Aedes albopictus? *PLoS Negl Trop Dis* 8(2):e2681.
9. Ledermann JP, et al. (2014) Aedes hensilli as a potential vector of Chikungunya and Zika viruses. *PLoS Negl Trop Dis* 8(10):e3188.
10. Aron JL, May RM (1982) The population dynamics of malaria. *The Population Dynamics of Infectious Diseases: Theory and Applications*, ed Anderson RM (Springer, Boston), pp 139–179.
11. Rogers DJ (1988) A general model for the African trypanosomiases. *Parasitology* 97(Pt 1): 193–212.
12. Lord CC, Woolhouse ME, Rawlings P, Mellor PS (1996) Simulation studies of African horse sickness and Culicoides imicola (Diptera:Ceratopogonidae). *J Med Entomol* 33(3):328–338.
13. Turner J, Bowers RG, Baylis M (2013) Two-host, two-vector basic reproduction ratio (R(0)) for bluetongue. *PLoS One* 8(1):e53128.
14. Wong P-SJ, Li MZ, Chong CS, Ng LC, Tan CH (2013) Aedes (Stegomyia) albopictus (Skuse): A potential vector of Zika virus in Singapore. *PLoS Negl Trop Dis* 7(8):e2348.
15. Chouin-Carneiro T, et al. (2016) Differential susceptibilities of Aedes aegypti and Aedes albopictus from the Americas to Zika virus. *PLoS Negl Trop Dis* 10(3):e0004543.
16. Diagne CT, et al. (2015) Potential of selected Senegalese Aedes spp. mosquitoes (Diptera: Culicidae) to transmit Zika virus. *BMC Infect Dis* 15:492.
17. Ponlawat A, Harrington LC (2005) Blood feeding patterns of Aedes aegypti and Aedes albopictus in Thailand. *J Med Entomol* 42(5):844–849.
18. Farjana T, Tuno N (2013) Multiple blood feeding and host-seeking behavior in Aedes aegypti and Aedes albopictus (Diptera: Culicidae). *J Med Entomol* 50(4):838–846.
19. Rogers DJ, Randolph SE (2006) Climate change and vector-borne diseases. *Adv Parasitol* 62:345–381.
20. Smith DL, et al. (2012) Ross, Macdonald, and a theory for the dynamics and control of mosquito-transmitted pathogens. *PLoS Pathog* 8(4):e1002588.
21. Foy BD, et al. (2011) Probable non-vector-borne transmission of Zika virus, Colorado, USA. *Emerg Infect Dis* 17(5):880–882.
22. Hayes EB (2009) Zika virus outside Africa. *Emerg Infect Dis* 15(9):1347–1350.
23. Berthet N, et al. (2014) Molecular characterization of three Zika flaviviruses obtained from sylvatic mosquitoes in the Central African Republic. *Vector Borne Zoonotic Dis* 14(12):862–865.
24. Kokernot RH, Casaca VM, Weinbren MP, McIntosh BM (1965) Survey for antibodies against arthropod-borne viruses in the sera of indigenous residents of Angola. *Trans R Soc Trop Med Hyg* 59(5):563–570.
25. Geser A, Henderson BE, Christensen S (1970) A multipurpose serological survey in Kenya. 2. Results of arbovirus serological tests. *Bull World Health Organ* 43(4):539–552.
26. Henderson BE, Kirya GB, Hewitt LE (1970) Serological survey for arboviruses in Uganda, 1967-69. *Bull World Health Organ* 42(5):797–805.
27. Pond WL (1963) Arthropod-borne virus antibodies in sera from residents of South-East Asia. *Trans R Soc Trop Med Hyg* 57:364–371.
28. Marchette NJ, Garcia R, Rudnick A (1969) Isolation of Zika virus from Aedes aegypti mosquitoes in Malaysia. *Am J Trop Med Hyg* 18(3):411–415.
29. Olson JG, Ksiazek TG, Suhandiman, Triwibowo (1981) Zika virus, a cause of fever in Central Java, Indonesia. *Trans R Soc Trop Med Hyg* 75(3):389–393.
30. Smithburn KC, Taylor RM, Rizk F, Kader A (1954) Immunity to certain arthropod-borne viruses among indigenous residents of Egypt. *Am J Trop Med Hyg* 3(1):9–18.
31. Bastos L, et al. (2016) Zika in Rio de Janeiro: Assessment of basic reproductive number and its comparison with dengue. *bioRxiv*, 10.1101/055475.
32. Nishiura H, Mizumoto K, Villamil-Gómez WE, Rodríguez-Morales AJ (2016) Preliminary estimation of the basic reproduction number of Zika virus infection during Colombia epidemic, 2015-2016. *Travel Med Infect Dis* 14(3):274–276.
33. Bhatt S, et al. (2013) The global distribution and burden of dengue. *Nature* 496(7446): 504–507.
34. Paz S, Semenza JC (2016) El Niño and climate change–contributing factors in the dispersal of Zika virus in the Americas? *Lancet* 387(10020):745.
35. Faria NR, et al. (2016) Zika virus in the Americas: Early epidemiological and genetic findings. *Science* 352(6283):345–349.
36. Muñoz ÁG, Thomson MC, Goddard L, Aldighieri S (2016) Analyzing climate variations at multiple timescales can guide Zika virus response measures. *Gigascience* 5(1):41.
37. Guis H, et al. (2012) Modelling the effects of past and future climate on the risk of bluetongue emergence in Europe. *J R Soc Interface* 9(67):339–350.
38. NVBDCP (2016) Dengue Cases and Deaths in India Since 2010. Available at nvbdcp.gov.in/den-cd.html. Accessed November 28, 2016.
39. Gould EA, Solomon T (2008) Pathogenic flaviviruses. *Lancet* 371(9611):500–509.
40. Medlock JM, et al. (2012) A review of the invasive mosquitoes in Europe: Ecology, public health risks, and control options. *Vector Borne Zoonotic Dis* 12(6):435–447.
41. Lourenço J, Recker M (2014) The 2012 Madeira dengue outbreak: Epidemiological determinants and future epidemic potential. *PLoS Negl Trop Dis* 8(8):e3083.
42. Messina JP, et al. (2016) Mapping global environmental suitability for Zika virus. *eLife* 5:5.
43. Alex Perkins T, Siraj AS, Ruktanonchai CW, Kraemer MU, Tatem AJ (2016) Model-based projections of Zika virus infections in childbearing women in the Americas. *Nat Microbiol* 1(9):16126.
44. Monaghan AJ, et al. (2016) On the seasonal occurrence and abundance of the Zika virus vector mosquito Aedes Aegypti in the contiguous United States. *PLoS Curr* 8:8.
45. Guo XX, et al. (2016) Culex pipiens quinquefasciatus: A potential vector to transmit Zika virus. *Emerg Microbes Infect* 5(9):e102.
46. Fernandes RS, et al. (2016) Culex quinquefasciatus from Rio de Janeiro is not competent to transmit the local Zika virus. *PLoS Negl Trop Dis* 10(9):e0004993.
47. Huang YJ, et al. (2016) Culex species mosquitoes and Zika virus. *Vector Borne Zoonotic Dis* 16(10):673–676.
48. Scott TW, Morrison A (2003) Aedes aegypti density and the risk of dengue-virus transmission. *Ecological Aspects for Application of Genetically Modified Mosquitoes*, eds Takken W, Scott TW (Frontis, Dordrecht, The Netherlands), Vol 2, pp 187–206.
49. Ferguson NM, et al. (2016) EPIDEMIOLOGY. Countering the Zika epidemic in Latin America. *Science* 353(6297):353–354.
50. Bogoch II, et al. (2016) Potential for Zika virus introduction and transmission in resource-limited countries in Africa and the Asia-Pacific region: A modelling study. *Lancet Infect Dis* 16(11):1237–1245.
51. Kraemer MUG, et al. (2015) The global distribution of the arbovirus vectors Aedes aegypti and Ae. albopictus. *eLife* 4:e08347.
52. Fan Y, van den Dool H (2008) A global monthly land surface air temperature analysis for 1948–present. *J Geophys Res* 113(D1):D01103.
53. Schneider U, et al. (2014) GPCC's new land surface precipitation climatology based on quality-controlled in situ data and its role in quantifying the global water cycle. *Theor Appl Climatol* 115(1):15–40.
54. Almeida APG, et al. (2005) Bioecology and vectorial capacity of Aedes albopictus (Diptera: Culicidae) in Macao, China, in relation to dengue virus transmission. *J Med Entomol* 42(3):419–428.
55. Tawatsin A, Thavara U (2010) Dengue haemorrhagic fever in Thailand: Current incidence and vector management. *Vector Biology, Ecology and Control*, ed Atkinson PW (Springer, Dordrecht, The Netherlands), pp 113–125.
56. Craig MH, Snow RW, le Sueur D (1999) A climate-based distribution model of malaria transmission in sub-Saharan Africa. *Parasitol Today* 15(3):105–111.
57. Kindhauser MK, Allen T, Frank V, Santhana RS, Dye C (2016) Zika: The origin and spread of a mosquito-borne virus. *Bull World Health Organ* 94(9):675–686C.
58. Liu-Helmersson J, Stenlund H, Wilder-Smith A, Rocklöv J (2014) Vectorial capacity of Aedes aegypti: Effects of temperature and implications for global dengue epidemic potential. *PLoS One* 9(3):e89783.
59. Scott TW, et al. (2000) Longitudinal studies of Aedes aegypti (Diptera: Culicidae) in Thailand and Puerto Rico: Blood feeding frequency. *J Med Entomol* 37(1):89–101.
60. Scott TW, et al. (1993) Blood-feeding patterns of Aedes aegypti (Diptera: Culicidae) collected in a rural Thai village. *J Med Entomol* 30(5):922–927.
61. Sivan A, Shriram AN, Sunish IP, Vidhya PT (2015) Host-feeding pattern of Aedes aegypti and Aedes albopictus (Diptera: Culicidae) in heterogeneous landscapes of South Andaman, Andaman and Nicobar Islands, India. *Parasitol Res* 114(9):3539–3546.
62. Kamgang B, Nchoutpouen E, Simard F, Paupy C (2012) Notes on the blood-feeding behavior of Aedes albopictus (Diptera: Culicidae) in Cameroon. *Parasit Vectors* 5:57.
63. Richards SL, Ponnusamy L, Unnasch TR, Hassan HK, Apperson CS (2006) Host-feeding patterns of Aedes albopictus (Diptera: Culicidae) in relation to availability of human and domestic animals in suburban landscapes of central North Carolina. *J Med Entomol* 43(3):543–551.
64. Faraji A, et al. (2014) Comparative host feeding patterns of the Asian tiger mosquito, Aedes albopictus, in urban and suburban Northeastern USA and implications for disease transmission. *PLoS Negl Trop Dis* 8(8):e3037.
65. Delatte H, et al. (2010) Blood-feeding behavior of Aedes albopictus, a vector of Chikungunya on La Réunion. *Vector Borne Zoonotic Dis* 10(3):249–258.
66. Andraud M, Hens N, Marais C, Beutels P (2012) Dynamic epidemiological models for dengue transmission: A systematic review of structural approaches. *PLoS One* 7(11):e49085.
67. Brady OJ, et al. (2013) Modelling adult Aedes aegypti and Aedes albopictus survival at different temperatures in laboratory and field settings. *Parasit Vectors* 6:351.
68. McLean DM, et al. (1974) Vector capability of Aedes aegypti mosquitoes for California encephalitis and dengue viruses at various temperatures. *Can J Microbiol* 20(2):255–262.
69. Musso D, et al. (2015) Detection of Zika virus in saliva. *J Clin Virol* 68:53–55.